Published in final edited form as:
Langmuir. 2013 January 8; 29(1): 337–343. doi:10.1021/la3039329.

Interaction forces between DPPC bilayers on glass

Raquel Orozco-Alcaraz and **Tonya L. Kuhl***
University of California Davis. Department of Chemical Engineering and Materials Science, One Shields Avenue, Davis CA 95616

Abstract

The Surface Force Apparatus (SFA) was utilized to obtain force-distance profiles between silica supported membranes formed by Langmuir-Blodgett deposition of 1,2-dipalmitoyl-*sn*-glycero-3-phosphocholine (DPPC). In the absence of a membrane, a long range electrostatic and short range steric repulsion is measured due to deprotonation of silica in water and roughness of the silica film. The electrostatic repulsion is partially screened by the lipid membrane and a van der Waals adhesion comparable to that measured with well packed DPPC membranes on mica is measured. This finding suggest that electrostatic interactions due to the underlying negatively charged silica are likely present in other systems of glass supported membranes. In contrast, the charge of an underlying mica substrate is almost completely screened when a lipid membrane is deposited on the mica. The difference in the two systems is attributed to stronger physisorption of zwitterionic lipids to molecularly smooth mica compared to rougher silica.

Keywords

lipid bilayer; force spectroscopy; monolayer; biosensor; interferometry; vesicle

INTRODUCTION

Due to the complexity of cell membranes, biophysical studies have primarily focused on model membrane systems of reduced complexity in order to elucidate the fundamental thermodynamics and physics of membrane interactions. For example, lipids and their self-organizing structures have been broadly used as models of cellular membranes and studied for their potential in biosensor applications[1]. In this work we compare the interaction forces between supported membranes composed of one of the most commonly studied phospholipids, DPPC on two different supports; molecularly smooth but chemically inert mica versus more functional and broadly used silica or glass.

There are a plethora of techniques used to study membranes, however relatively few provide a measure of membrane-membrane interactions[2–3]. One of the first methods developed relied on changes in the spacing between membranes in multilamellar stacks under osmotic stress to extract the repulsive interactions between membranes[4–5]. Such studies provided unprecedented understanding of the role of membrane undulations and hydration. The use of small and wide angle x-ray and neutron scattering also provided high resolution density distributions and average packing of lipids in the membrane to be obtained.[6–9] More

*tlkuhl@ucdavis.edu.

ASSOCIATED CONTENT

Supporting Information Available: Part 1: Experimental comparison between multilayer matrix model and the 3-layer and 5-layer multiple beam interferometry models. Fluorescent microscopy images of supported DPPC membranes on mica and silica coated mica. Part 2: Fluorescent images of DPPC bilayers on mica and silica-coated mica. This material is available free of charge via the Internet at http://pubs.acs.org

recently, the bioforce probe based on micropipette aspiration of giant unilamellar vesicles has been used to measure membrane-membrane interactions. Initially used to study membrane tension and area compressibility by measuring changes in membrane shape as a function of pipette suction pressure, the use of opposing membranes and/or a force sensing red blood cell expanded the measuring capability to detect weak attractive interactions as well as biological specificity interactions such as ligand-receptor binding[2, 10–12]. In terms of substrate supported membranes, Atomic Force Microscopy (AFM)[13] is widely used to measure membrane topology, but only sparingly used to measure membrane-membrane interactions due to challenges in forming a membrane on silicon nitride tips.[14–16] Chemically functionalizing the tip with gold and a hydrophobic mercapto undecanol has been shown to promote spontaneous vesicle fusion, yielding a supported lipid monolayer appropriate for measuring membrane-membrane interactions.[15]

The most widely used and versatile technique for measuring membrane-membrane interactions is the Surface Force Apparatus, which provides force-distance profiles with 1Å resolution in distance, 10pN in force, and visualization of the area of contact between two macroscopic membrane coated surfaces.[2, 17–22] Traditionally, SFA employs mica, a molecularly smooth and widely used solid support for force spectroscopy and fluorescence microscopy measurements. However, membrane based biosensors typically use silica or glass substrates; in part due to the fact that silica is readily available, cheap, easily chemically modified, optically transparent, and less sensitive to surface damage[23–25]. It is, thus, important to establish the typical conditions present (e.g. charge density, hydrophobicity, steric interactions, etc.) for a bilayer immobilized on silica and thus how a silica supported membrane interacts with materials in the environment (e.g. particles, proteins, cells, etc.) for applications. Moreover, there is a large effort to develop models to recapitulate integral membrane proteins in supported membranes for controlled biophysical studies[26–28]. In order to study the interaction of membranes with transmembrane proteins, it is necessary to prevent deleterious interactions of the embedded protein with the underlying inorganic support. Hydrophilic polymer cushions are actively being pursued as a means to provide a highly hydrated, soft, flexible spacer between the substrate and the membrane to better mimic biological conditions and native function [24, 29–40] Grafting of polymers on silica is becoming routine. Follow on work will present studies of interaction forces of polymer cushioned membranes.[41]

Though the interaction between lipid bilayers immobilized on mica surfaces have been well documented, no work has reported measurements of membranes immobilized on silica using the SFA. In this work, we measure and analyze the interaction between two DPPC bilayers deposited on smooth silica thin-films. The silica (SiO_2) is deposited via electron beam deposition (e-beam) on mica to yield relatively smooth films (5Å rms). The resulting optical interferometer is analyzed using both the 5-layer multiple beam interferometry analytical solution and multiple matrix solution of the full optical system (see supplemental information). The results are compared to the interaction of bilayers immobilized directly on mica under similar conditions.

MATERIALS AND METHODS

Chemicals

1,2-dipalmitoyl-*sn*-glycero-3-phosphocholine (DPPC) (melting point 41°C) was purchased from Avanti Polar Lipids, Inc. (Alabaster, AL). Texas Red® 1,2-Dihexadecanoyl-sn-Glycero-3-Phosphoethanolamine, Triethylammonium Salt (TexasRed DHPE) was purchased from Life Technologies Corp. (Grand Island, NY). Lipids were dissolved in chloroform at a concentration of 1 mg/ml. KNO_3 was used as the monovalent electrolyte in all solutions.

The water used was purified with a MilliQ Gradient water purification system, with a resistivity of 18MΩ·cm.

Sample preparation

Silica-covered mica was prepared based on the procedures previously described by Vigil et al.[42] First, mica was cleaved to uniform thicknesses of 3 to 4 microns, and adhered to a clean mica backing sheet. A CHA e-beam evaporator SEC-600-RAP was then used to deposit SiO_2 onto the mica pieces. To ensure uniform deposition the samples were rotated in their planetaries and the raster was scanned at an amplitude of one fourth of the crucible's diameter. Films with approximately 500Å or 1000Å SiO_2 layers were deposited using the following operating conditions; base pressure of 10^{-6} torr, deposition pressure of 5×10^{-6} torr, filament current of 26mA, accelerating voltage of −10kV, and a deposition rate of ~1Å/s. After the SiO_2 was deposited, the SiO_2-covered mica pieces were flipped and adhered to a clean mica sheet and silver was evaporated onto the backside of the mica pieces. Samples were stored under vacuum in this configuration until use.

Supported lipid bilayers were prepared by Langmuir-Blodgett (LB) deposition using a temperature-controlled Wilhelmy Trough (Nima Coventry, UK) and assembled onto the back-silvered mica or SiO_2 coverd mica substrates glued onto cylindrical silica disks, a procedure described elsewhere.[43–44] Prior to lipid deposition the SiO_2-mica surfaces were placed under UV light for a total of 30 minutes in 10 minute increments to ensure cleanliness and surface hydroxylation. Both the inner and outer leaflets of DPPC were deposited at 45mN/m. The inner leaflet was deposited by raising the substrates vertically through a compressed DPPC monolayer at the air-water interface at a dipping speed of 1mm/min. The monolayer transfer ratio was 1.00±0.05 on mica and 0.97±0.05 on SiO_2-mica. Subsequently, the outer DPPC layer was deposited in a vertical geometry under similar conditions but at a faster deposition rate of 4mm/min to prevent desorption of the inner leaflet at the air-water interface. The transfer ratio for the outer monolayer was 1.00±0.05 on mica and 0.90±0.05 on SiO_2-mica. The pressure-area isotherms obtained were in agreement with those in literature.[45] To demonstrate the similar quality of the deposited DPPC membranes on mica and SiO_2-mica surfaces, fluorescence images of DPPC membranes containing 1mole% Texas Red DHPE are shown in the supplemental information. No fluorescent dye was incorporated into membranes for SFA experiments.

Atomic Force Microscopy (AFM)

AFM studies were done using the NEAT-ORU spectral imaging facility at the UC Davis campus with an Asylum Research (Santa Barbara, CA) MFP-3D AFM. Veeco SiliconNitride MSCT levers, k~=0.03, were used for imaging.

Surface Force Measurements

The SFA technique has been used extensively to measure interaction forces between surfaces[46–47]. After bilayers were deposited on the solid support, the surfaces were transferred and mounted into the SFA under water, a procedure detailed elsewhere[17]. The water in the SFA box was saturated with a speckle of DPPC to prevent lipid desorption from the substrate during the course of the measurements. After the surfaces were mounted, the SFA box was placed in a temperature controlled room at 25.0°C. A custom, automated SFA was used for convenient data collection[48]. The system enables constant and/or variable motor displacements via a computer controlled motor system. A sensitive CCD camera (Princeton SPEC-10:2K Roper Scientific, Trenton NJ) was interfaced with the spectrometer and computer acquisition system to allow automated wavelength determination of the fringes of equal chromatic order.

The separation distance analysis traditionally used for supported membranes on mica surfaces is to approximate the system as a symmetric 3-layer interferometer and use analytical solutions for the resulting optical interferometer. Other methods include a 5-layer analytical form and the multilayer matrix model (MMM) that can be used for asymmetric and more complicated optical systems. Immobilizing bilayers on mica-covered silica surface requires an extra set of symmetric layers in the interferometer and complicates the analysis of the separation distance. In the supplemental information for this work, we demonstrate that approximating the optical system using a simple 3-layer interferometer is insufficient, and can only be used as a first estimate of the separation distance. The difference between the results obtained using the 3-layer analytical method and MMM is ~13%, while the difference between the 5-layer analytical method and MMM is ~3.5% for separation distances less than 200Å. In this work the 5-layer analytical method was primarily employed. Membrane thickness at contact was determined using MMM.

RESULTS

AFM of SiO_2 covered mica

Figure 1A shows a representative AFM image of a ~1000Å-thick SiO_2 layer, e-beam deposited on mica hydrated in MilliQ water. Figure 1B shows the 3-dimensional profile that corresponds to image 1A. Image analysis gave a peak to valley roughness of 31±2Å for a hydrated film in bulk water (6±2Å rms). Similar surface quality was observed with dry films in air (results not shown). In all cases scans were recorded over different regions of the films and the scans were reproducible. Similar, but lower, values for the roughness of e-beam deposited SiO_2 thin films on mica were reported by Vigil et al. The surface quality of our films is also consistent with SFA measurements, where we found the SiO_2 films swelled slightly by 2.2% in water compared to their dry thickness (see supplemental information). Vigil et al. suggested the swelling was due to formation of protruding silica hairs or gel formation at the SiO_2-water interface. As the roughness of our SiO_2 film did not increase appreciably upon hydration, we attribute the 2.2% increase in film thickness to imbibing a small amount of water in defects within the SiO_2 film.

SiO_2 interaction in aqueous solution

Figure 2 shows the force-distance profile between two e-beam evaporated silica films on mica in ~0.5mM KNO_3 at pH 6. Contact, D=0, was defined as hard flattened contact in air ($F/R \geq 70$ mN/m). The force curve is characterized by two types of repulsive interactions: the expected long range electrostatic double layer interaction due to the negative charge of the silica film in water and a shorter-range steric interaction presumably due to surface roughness and hydration[49–50]. Theoretically and experimentally both electrostatic and steric/hydration interactions decay roughly exponentially. The silica surfaces were assumed to be symmetric, ie. the films had the same negative charge density or surface potential. The electrostatic interaction was then fitted by solving the nonlinear Poisson-Boltzmann (P-B) equation using a numerical algorithm developed by Grabbe and Horn.[51] The algorithm explicitly computes the electrostatic potential or constant surface charge between two flat surfaces using a relaxation method on a finite mesh. The Derjaguin approximation was used to convert from the energy between flats to force between crossed cylinders, $F/R = 2\pi E$. The solid lines are the P-B fits for a constant potential of $\psi = -107$mV and a constant surface charge of $\sigma = 9.2$mC/m^2. These results are in good agreement with previous studies where the magnitude of the negative surface potential of silica at pH = 7.5 was $\psi = -120$mV in 0.1mM NaCl.[23, 52] For the conditions here, pH~6, a lower charge density and zeta potential are expected.[53]

To better qualify the short-range interaction, the electrostatic contribution was subtracted from the measured force profile[43]. The remaining, steric portion of the interaction is shown in the Inset of Figure 2. The measured force profile deviates from a purely electrostatic interaction at short range, D<30Å, consistent with the AFM topography measurements in Figure 1. When an exponential is fit $F/R \sim \exp(D/L_c)$, we find that the characteristic length for this case is $L_c \sim 6$Å. The characteristic length is consistent with hydration of the silica interface and compression/interdigitation of protrusions of the opposing surfaces (6±2Å rms).[49–50] This additional repulsive contribution can possibly be explained by Valtiner at al., who suggested that this additional force is attributed to repulsive hydration and steric forces.[54–55] After hydration, no change in the interaction profile was detected over many days demonstrating that the films were stable. A similar short-range repulsion between silica films in water was observed by Vigil et al.,[42] but attributed to the extension of dangling Si-(-O-Si-)n-OH groups and formation of a silica gel.

Control measurements of DPPC bilayers on mica

Traditionally DPPE has been used as the inner leaflet layer in supported membrane experiments measured with the SFA. DPPE binds to mica through a strong electrostatic interaction and provides a stable hydrophobic surface upon which to deposit the outer lipid monolayer leaflet. Here, a symmetric DPPC bilayer was used instead as DPPC is one of the most commonly studied phospholipids and considered a better mimic of biological membranes.[23, 56] Before describing the results of the force-distance, F(D), measurements, it is important to establish an appropriate reference frame for the contact between the bilayer surfaces, which will define D=0. As in previous SFA measurements, we choose to define D=0 as contact between the membranes in the absence of hydration and protrusion effects.[17] In the case of DPPC membranes supported on mica, the hydrated thickness of the two outer monolayers, Δ, was determined at the end of each experiment by measuring the thickness change following drainage of the solution from the apparatus and removal of the two outer monolayers. From the measured thickness change relative to contact between the bilayers at a force of about 10mN/m, bilayer-bilayer contact, D=0, was defined as

$$D=\Delta-T \quad \text{(Eq. 1)}$$

The anhydrous bilayer thickness (T) was calculated from the known volumes occupied by the hydrocarbon chains and PC head group given by

$$T=2[2V_{hc}+V_{head}]/A \quad \text{(Eq. 2)}$$

where $V_{hc}=(27.4+26.9n)$ Å^3 is the average volume of a saturated n-carbon chain in the gel state[57], $V_{head}=324.5$Å^3 is the average head group volume of PC[58], and A is the deposited area per lipid. For example, the thickness of two outer DPPC monolayers deposited at A = 48 Å^2 per molecule (Π=45mN/m) is $T = 2[2(27.4 + 26.9x15) + 324.5]/48 = 49.4$Å. Typically, phosphotidylcholine membranes come into contact at separations of about 20–30Å depending on the compressive load.[17, 59] The thickness of the bilayer was assumed to remain constant during experiments. This is reasonable given that the DPPC monolayers (T_{mp} = 41°C) were deposited at room temperature in a close packed solid phase and no phase changes or density changes are expected to take place.

Figure 3A shows the measured force-distance profile between two DPPC bilayers immobilized on mica substrates in a monovalent solution of 0.5mM KNO_3 at room temperature. As can be seen, a very weak repulsion[60] is observed between the surfaces for separations below ~150Å followed by a strong, short-range repulsion at about 30Å. As

DPPC is zwitterionic, but overall neutral, we attribute the weak repulsion to a small level of residual charge from the mica surfaces or lipid membrane as the decay length is roughly consistent with the electrolyte concentration[60]. If fully dissociated, mica has a maximum surface charge density[46] of 50Å^2/e$^-$. The surface charge density or surface potential measured experimentally is dependent upon the type and concentration of electrolyte present in the solution. As shown in Figure 3A, the surface charge of the mica is almost completely damped after depositing a bilayer (with a low dielectric oil core) on the surface.[61] The almost-negligible electrostatic repulsion suggests reasonably strong electrostatic binding of DPPC lipid bilayer to mica. The electrostatic binding rises from the attractive interaction between the underlying, negatively charged mica substrate and the positively charged terminus of the zwitterionic headgroup. In contrast, no electrostatic repulsion is measured when the inner leaflet of the membrane is DPPE. Presumably the difference resides in the weaker physisorption and higher hydration of PC headgroups compared to PE headgroups[62].

Figure 3B illustrates the van der Waals adhesion between the DPPC bilayers with a magnitude of $A_{dh} = F_{ad}/R = -0.40 \pm 0.10$ mN/m at a separation of D = 30±3Å. In addition, the experimental data was compared to the theoretical Van der Waals interaction[17] $F=-AR/6D^2$ (dash line) with $A=(7\pm1)\times10^{-21}$J, with excellent agreement. The inset in Figure 3B is a semi-log plot of the short range repulsion between the membranes. An ever present hydration layer on the head groups and the thermal protrusions of lipids from the membrane are responsible for the short range repulsion. In addition, as suggested Marra and Israelachvili[17], the hydration of cations can also add to the repulsive force.

SFA measurements of DPPC bilayers immobilized in SiO_2

The measured transfer ratio of DPPC bilayer on the SiO_2 coated mica surfaces was 0.97±0.05 for the inner leaflet and 0.90±0.05 for the outer leaflet. This result corroborates an earlier reflectivity studies that showed the formation of a well packed membrane with near complete coverage on a silica surface using the LB deposition technique.[63] Fluorescence images of DPPC membranes containing 1mole% Texas Red DHPE on SiO_2 coated mica are shown in the supplemental information. As evidenced by fluorescence microscopy well packed membranes are present at the micron scale. However, the presence of small defects cannot be ruled out from such measurements. The lower transfer ratios of lipid monolayers obtained on silica to mica also suggest that the membranes on silica contain a higher number of defects, which is consistent with the significant electrostatic repulsion measured with silica supported DPPC membranes described in the next section. Bassereau and Pincet demonstrated that lipids in the inner leaflet can desorb during the deposition of the outer leaflet monolayer, thereby resulting in lower transfer ratios and holes in the bilayer. The holes span the thickness of the bilayer due to the high energy of exposing hydrophobic chains to water. The adsorption energy of a DPPC lipid to SiO_2 vs mica can be readily estimated from their transfer ratios using:[64]

$$E_a/kT=(\alpha\, a_m\, \gamma_{DPPC}/kT)-ln(\rho) \quad \text{(Eq. 3)}$$

where E_a is the adsorption energy, k is the Boltzmann's constant, T is the temperature, a_m is the molecular area of DPPC (a_m= 45 Å^2 at Π_{DPPC} =45mN/m),[65–66] α is a correlation coefficient, and γ_{DPPC} is the surface tension of DPPC at the air-water interface defined as γ_{DPPC} = 72mN/m − Π_{DPPC}.[67] The ratio between the total surface covered by holes and bilayer is $\rho = x/(1-x)$, where x can be found from the transfer ratio, x =(1−R)/2.[64] To calculate the adhesion energy, we assume α=0.7, the correlation value measured for DMPE on mica[64]. This yields an adsorption energy of a DPPC bilayer on silica of $E_a \sim 1kT$ (for R=0.90) vs. an adsorption energy on mica of $E_{a,min} \sim 3kT$ (for R=0.99). This difference confirms the lower adsorption energy of DPPC bilayers on silica than mica.

Figure 4A shows the measured force-distance profile of DPPC bilayers immobilized on silica substrates under different ionic strengths (0.5 and 1.5mM KNO_3). The reduction of the long-range repulsion with increased salt concentration clearly demonstrates that the interaction is electrostatic. As mentioned earlier, the head groups of the lipid bilayers are zwitterionic but overall neutral in charge. Thus, the long range electrostatic force is due to the underlying, negatively charged SiO_2 coated mica substrates. To clearly delineate the electrostatic contribution of the SiO_2 films in the measured force profile, the reference frame, D=0, is based on SiO_2-SiO_2 contact in 0.5mM KNO_3 aqueous solution rather than DPPC-DPPC membrane contact. The distance-shift was based on the contact before (SiO_2-SiO_2 in water) and after the bilayers were immobilized on silica using MMM to determine the thickness of the membranes. MMM was used in this case to ensure correct membrane thickness measurements. Equation 1 was also employed to observe consistency in outer layer thickness between immobilized bilayers on silica vs. mica. Interestingly, we observed an additional shift of 20Å in the thickness estimated by draining the SFA of water and removal of the outer DPPC monolayer leaflets compared to studies on mica. We attribute this to some loss of the inner layer leaflets of the membranes immobilized on silica. Removal of more than the outer two leaflets demonstrates a weaker physisorption of the inner leaflet to silica as compared to mica again consistent with the difference in the estimated adsorption energy (Eq. 3).

The electrostatic repulsion was fit using the Poisson-Boltzmann (P-B) equation at the two salt concentrations. The electrostatic potential decreases slightly as the electrolyte concentration increases, and the potential is lower in the presence of a membrane (Figure 2). The significant electrostatic repulsion is likely due to small holes in the membrane, and therefore, less screening of the underlying substrate charge by the supported membrane. Adhesion is again observed when the surfaces are separated. The adhesion is comparable between the two salt concentrations with a magnitude of about −0.65mN/m. This is in very good agreement with the expected VDW adhesion between DPPC bilayers.[17] No additional attraction or adhesion from hydrophobic interactions was detected. This is consistent with the formation of membrane spanning holes as observed by AFM[64, 68–69]. We further comment that the measured adhesion is identical to the measured adhesion of DPPC membranes on mica once the small electrostatic contribution is accounted for, −(0.40+0.20)mN/m.

After subtracting the electrostatic contribution (Figure 4B) the remaining short range repulsion is “softer” compared to when the bilayer is supported on mica substrates. This softer repulsion is consistent with the increase in surface roughness.[54–55] For this figure, D=0 was defined as the contact between DPPC bilayers for ease of comparison to data shown in Figure 3. To obtain D=0, the thickness of two DPPC membranes was determined using Equation 2 and subtracted from the total thickness as determined using MMM and the contact wavelengths in the presence and absence of the membranes.

CONCLUSIONS

Though the interaction between lipid bilayers immobilized on mica surfaces have been well documented, much less work has been done on bilayers immobilized on silica. The closest system was a measurement of a lipid bilayer on mica with a bare silica surface by Anderson et al.[23] The measured profile between a mica supported membrane and bare silica surface demonstrated that a long range repulsion force, attributed to residual double layer potential, and short-range repulsive thermal undulation forces were the dominant interactions.

The structure of DPPC membranes is similar on mica or silica surfaces as ascertained by fluorescence microscopy (supplemental information), however it is likely that silica

supported membranes contain more holes as indicated by reduced transfer ratios.. The measured forces between DPPC bilayers immobilized on silica or mica are also similar, with the exception of a stronger electrostatic repulsive force present when silica is used. A summary of the forces and observations made in these experiments is enumerated next. First, the most important difference between the interaction of bilayers immobilized on mica and bilayers immobilized on silica is the presence of a strong electrostatic force when silica is used. We attribute this force to holes in silica supported membranes due to the weaker physisorption of lipids to the silica substrate and the hydrated surface roughness of the silica. These defects are below the resolution of fluorescence microscopy. Second, a van der Waals attraction consistent with well-packed membranes is measured upon membrane separation. In Figure 3B and 4B, the theoretical Van Der Waals interaction, $F=-AR/6D^2$ with $A=(7\pm1)\times10^{-21}$J is plotted against the experimental results (dashed lines for both figures). For silica $D_{eq}=34\pm3$Å, which is slightly greater than the equilibrium distance for mica ($D_{eq}=30\pm3$Å) due to the greater fluctuations in the more hydrated membrane and roughness of the underlying silica support. The magnitude of adhesion force between membranes immobilized on silica, A_{dh}, is in agreement with theoretical predictions and previous measurements of DPPC membranes supported on inner leaflets of DPPC[17]. The adhesion is comparable between the two salt concentrations at about 0.65mN/m. Third, membranes on silica appear slightly more compressible due to the softer/rougher underlying silica layer. Fourth, the physisorption of the inner DPPC leaflet to silica is weaker than to mica and can be quantified by the lower transfer ratios during Langmuir Blodgett deposition.

In particular, the presence of an unexpected electrostatic interaction when membranes are supported on silica and presence of holes in the membrane could be important in biophysical membrane studies on glass and biosensor applications where selective binding of ligands or proteins to membranes is important.

Supplementary Material

Refer to Web version on PubMed Central for supplementary material.

Acknowledgments

This work was supported by NSF Chemistry Division through grant CHE-0957868 and from the NIH Training Grant in Biomolecular Technology awarded by the Designated Emphasis in Biotechnology at UC Davis. We also thank Daniel Kienle and Dennis Mulder for assistance with MMM modeling, William Chan for fluorescent microscopy measurements, and Gwen Schuman for her contributions in transfer ratio measurements.

References

1. Sackmann E. Supported Membranes: Scientific and Practical Applications. Science. 1996; 271(5245):43–48. [PubMed: 8539599]
2. Leckband D, IJ. Intermolecular Forces in Biology. Quarterly Reviews of Biophysics. 2001; 34(2): 105–267. [PubMed: 11771120]
3. Claesson PE, Bergeron TV, et al. Techniques for measuring surface forces. ADVANCES IN COLLOID AND INTERFACE SCIENCE. 1996; 67:119–183.
4. Rand RP, PVA. Hydration forces between phospholipid bilayers. Biochim Biophys Acta. 1989; 988(3):351–376.
5. Safinya CR, Roux D, Smith GS, Sinha SK, Dimon P, Clark NA, Bellocq AM. Steric Interactions in a Model Multimembrane System: A Synchrotron X-Ray Study. Phys Rev Lett. 1986:2718–2721. [PubMed: 10033843]
6. Parsegian VA, Fuller N, Rand RP. The role of long range forces in ordered arrays of tobacco mosaic virus. Nature. 1979; 259:632–635. [PubMed: 1250412]

7. Caffrey MB, Bilderback DH. Realtime X-ray diffraction using synchrotron radiation: system characterization and applications. Nucl Instrum Meth. 1983; 208:495–510.
8. Nagle J, T-NS. Structure of lipid bilayers. BIOCHIMICA ET BIOPHYSICA ACTA-REVIEWS ON BIOMEMBRANES. 2000; 1469(3):159–195.
9. Petrache H, GN, Tristram-Nagle S, et al. Interbilayer interactions from high-resolution x-ray scattering. PHYSICAL REVIEW E. 1998; 57(6):7014–7024.
10. Evans E, KDJ, Rawicz W, et al. Interactions between polymer-grafted membranes in concentrated solutions of free polymer. LANGMUIR. 1996; 12(12):3031–3037.
11. Evans E, ND. Physical Properties of Surfactant Bilayer-Membranes - Thermal Transitions, Elasticity, Rigidity, Cohesion, and Colloidal Interactions. JOURNAL OF PHYSICAL CHEMISTRY. 1987; 91(16):4219–4228.
12. Evans E, RK, Merkel R. Sensitive Force Technique To Probe Molecular Adhesion and Structural Linkages at Biological Interfaces. BIOPHYSICAL JOURNAL. 1995; 68(6):2580–2587. [PubMed: 7647261]
13. Alessandrini A, FP. AFM: a versatile tool in biophysics. MEASUREMENT SCIENCE & TECHNOLOGY. 2005; 16(6):R65–R92.
14. Garcia-Manyes S, Sanz F. Nanomechanics of lipid bilayers by force spectroscopy with AFM: A perspective. Biochimica et Biophysica Acta. 2010:741–749. [PubMed: 20044974]
15. Pera I, Stark R, Kappl M, Butt HJ, Benfenati F. Using the Atomic Force Microscope to Study the Interaction between Two Solid Supported Lipid Bilayers and the Influence of Synapsin I. Biophysical Journal. 2004; 87(4):2446–2455. [PubMed: 15454442]
16. Richter RP, Brisson A. Characterization of lipid bilayers and protein assemblies supported on rough surfaces by atomic force microscopy. Langmuir. 2003; 19:1632–1640.
17. Marra J, Israelachvili J. Direct Measurements of Forces between Phosphatidylcholine and Phosphatidylethanolamine Bilayers in Aqueous Electrolyte Solutions. Biochemistry. 1985; 24:4608–4618. [PubMed: 4063343]
18. Orozco-Alcaraz R, KTL. Impact of membrane Fluidity on Steric Stabilization by Lipopolymers. Langmuir. 2012; 28:7470–7475. [PubMed: 22537191]
19. Moore NW, Kuhl TL. Bimodal Polymer Mushrooms: Compressive Forces and Specificity toward Receptor Surfaces. Langmuir. 2006; 22:8485–8491. [PubMed: 16981767]
20. Helm CA, Israelachvili JN, McGuiggan PM. ROLE OF HYDROPHOBIC FORCES IN BILAYER ADHESION AND FUSION. Biochemistry. 1992; 31(6):1794–1805. [PubMed: 1737032]
21. Leckband DE, Helm CA, Israelachvili J. Role of calcium in the adhesion and fusion of bilayers. Biochemistry. 1993; 32(4):1127–1140. [PubMed: 8424941]
22. Sheth SR, Leckband D. Measurements of attractive forces between proteins and end-grafted poly(ethylene glycol) chains. Proceedings of the National Academy of Sciences of the United States of America. 1997; 94(16):8399–8404. [PubMed: 9237988]
23. Anderson TH, MY, Weirich KL, Zeng H, Fygenson D, Israelachvili JN. Formation of Supported Bilayers on Silica Substrates. American Chemical Society. 2009; 25(12):6997–7005.
24. Sackmann E. Supported Membranes: Scientific and Practical Applications. Science. 1996; 271(5245):43–48. [PubMed: 8539599]
25. Tamm LK, MHM. Supported phospholipid bilayers. Biophys J. 1985; 47:105–113. [PubMed: 3978184]
26. Siegel DP. Inverted micellar intermediates and the transitions between lamellar, cubic, and inverted hexagonal lipid phases. II. Implications for membrane-membrane interactions and membrane fusion. Biophysical Journal. 1986; 49(6):1171–1183. [PubMed: 3719075]
27. Paulsson M. Basement Membrane Proteins: Structure, Assembly, and Cellular Interactions. Critical Reviews in Biochemistry and Molecular Biology. 1992; 27(1–2):93–127. [PubMed: 1309319]
28. Lorenza B, KR, Sunnicka E, Geila B, Janshoff A. Colloidal probe microscopy of membrane–membrane interactions: From ligand–receptor recognition to fusion events. Biophysical Chemistry. 2010; 150(1–3):54–63. [PubMed: 20219280]
29. Tanaka M, SE. Polymer-Supported membranes as models of the cell surface. Nature. 2005; 437(29):656–663. [PubMed: 16193040]

30. Knoll W, Bender K, Förch R, Frank C, Götz H, Heibel C, Jenkins T, Jonas U, Kibrom A, Kügler R. Polymer-Tethered Bimolecular Lipid Membranes. Polymer Membranes/Biomembranes. 2010; 224:87–111.
31. Spinke J, Yang J, Wolf H, Liley M, Ringsdorf H, Knoll W. Polymer-supported bilayer on a solid substrate. Biophysical Journal. 1992; 63(6):1667. [PubMed: 19431869]
32. Chi L, Anders M, Fuchs H, Johnston R, Ringsdorf H. Domain structures in Langmuir-Blodgett films investigated by atomic force microscopy. Science. 1993; 259(5092):213. [PubMed: 17790988]
33. Majewski J, WJ, Park C, Seitz M, Israelachvili J, Smith G. Structural studies of polymer-cushioned lipid bilayers. Biophysical Journal. 1998; 75(5):2363–2367. [PubMed: 9788931]
34. Wong JY, MJ, Seitz M, Park CK, Israelachvili JN, Smith GS. Polymer-cushioned bilayers. I. A structural study of various preparation methods using neutron reflectometry. Biophysical Journal. 1999; 77(3):1445–1457. [PubMed: 10465755]
35. Baumgart T, OA. Polysaccharide-supported planar bilayer lipid model membranes. Langmuir. 2003; 19(5):1730–1737.
36. Wang L, SM, Möhwald H. Lipids coupled to polyelectrolyte multilayers: ultraslow diffusion and the dynamics of electrostatic interactions. The Journal of Physical Chemistry B. 2002; 106(35): 9135–9142.
37. Smith HL, JMS, Vidyasagar A, Saiz J, Watkins E, Toomey R, Hurd AJ, Majewski J. Model lipid membranes on a tunable polymer cushion. Physical Review Letters. 2009; 102(22):228102. [PubMed: 19658904]
38. Wagner ML, TLK. Tethered polymer-supported planar lipid bilayers for reconstitution of integral membrane proteins: silane-polyethyleneglycol-lipid as a cushion and covalent linker. Biophysical Journal. 2000; 79(3):1400–1414. [PubMed: 10969002]
39. Naumann CA, PO, Lehmann T, Rühe J, Knoll W, Frank CW. The polymer-supported phospholipid bilayer: tethering as a new approach to substrate-membrane stabilization. Biomacromolecules. 2002; 3(1):27–35. [PubMed: 11866552]
40. Sinner EK, KW. Functional tethered membranes. Current opinion in chemical biology. 2001; 5(6): 705–711. [PubMed: 11738182]
41. El-khouri RJ, BDA, Watkins EB, Kim CY, Miller CE, Patten TE, Parikh AN, Kuhl TL. pH Responsive Polymer Cushions for Probing Membrane Environment Interactions. Nanoletters. 2011; 11(5):2169–2172.
42. Vigil G, XZ, Steinberg S, Israelachvili J. Interactions of Silica Surfaces. Colloid and Interface Science. 1994; 165:367–385.
43. Kuhl TL, Leckband DE, Lasic DD, Israelachvili JN. Modulation of Interaction Forces Between Bilayers Exposing Short-Chained Ethylene Oxide Headgroups. Biophysical Journal. 1994; 66:1479–1487. [PubMed: 8061197]
44. Kuhl, TL.; Leckband, DE.; Lasic, DD.; Israelachvili, JN. Modulation and Modeling of Interaction Forces Between Lipid Bilayers Exposing Terminally Grafted Polymer Chains. In: Lasic, DaM; Frank, editors. Stealth Liposomes. CRC Press; 1995. p. 73-91.
45. Klopfer KJ, VTK. Isotherms of Dipalmitoylphosphatidylcholine (DPPC) Monolayers: Features Revealed and Features Obscured. JOURNAL OF COLLOID AND INTERFACE SCIENCE. 1996; 182:220–229.
46. Israelachvili JN, Adams GE. Measurement of Forces between Two Mica Surfaces in Aqueous Electrolyte Solutions in the Range 0–100 nm. Chem Soc, Faraday Trans. 1978; 74:975–1001.
47. Israelachvili J. Thin film studies using multiple beam interferometry. J Colloid Interface Science. 1973; 44:259.
48. Moore NW, Mulder Dennis J, Kuhl Tonya L. Adhesion from Tethered Ligand-Receptor Bonds with Microsecond Lifetimes. Langmuir. 2008; 24:1212–1218. [PubMed: 18081329]
49. Valle-Delgado JJ, Molina-Bolivar JA, Galisteo-Gonzalez F, Galvez-Ruiz GMJ, Feiler A. Hydration forces between silica surfaces: Experimental data and predictions from different theories. Journal of Chemical Physics. 2005; 123(3)

50. Drelich J, Long J, Xu Z, Masliyah J, White CL. Probing colloidal forces between a Si3N4 AFM tip and single nanoparticles of silica and alumina. Journal of Colloid and Interface Science. 2006; 303(2):627–638. [PubMed: 16942778]
51. Grabbe A, HRG. Double-Layer and Hydration Forces Measured between Silica Sheets Subjected to Various Surface Treatments. Journal of Colloid and Interface Science. 1993; 157(2):375–383.
52. Scales PJ, GF, Healy TW. Electrokinetics of the Silica-Solution Interface: A Flat Plate Streaming Potential Study. Langmuir. 1992; 8(3):965–974.
53. Schwer C, KE. Electrophoresis in Fused-Silica Capillaries: The Influence of Organic Solvents on the Electroosmotic Velocity and the Zeta Potential. ANALYTICAL CHEMISTRY. 1991; 63(17): 1801–1807.
54. Valtiner M, Banquy X, Kristiansen K, Greene GW, Israelachvili JN. The Electrochemical Surface Forces Apparatus: The Effect of Surface Roughness, Electrostatic Surface Potentials, and Anodic Oxide Growth on Interaction Forces, and Friction between Dissimilar Surfaces in Aqueous Solutions. Langmuir. 2012; 28:13080–13093. [PubMed: 22877582]
55. Valtiner M, Kristiansen K, Greene GW, Israelachvili JN. Effect of Surface Roughness and Electrostatic Surface Potentials on Forces Between Dissimilar Surfaces in Aqueous Solution. Advanced Materials. 2011; 23:2294–2299. [PubMed: 21608041]
56. Castellana ET, Cremer PS. Solid supported lipid bilayers: From biophysical studies to sensor design. Surface Science Reports. 2006; 61:429–444.
57. Tanford C. Micelle Shape and Size. The Journal of Physical Chemistry. 1972; 76(21)
58. Small DM. Phase equilibria and structure of dry and hydrated egg lecithin. Journal of Lipid Research. 1967; 8:551–557. [PubMed: 6057484]
59. Kuhl TL, Berman AD, Hui SW, Israelachvili JN. Part 1. Direct Measurement of Depletion Attraction and Thin Film Viscosity between Lipid Bilayers in Aqueous Polyethylene Glycol Solutions. Macromolecules. 1998; 31:8250–8257.
60. Pincet F, Cribier S, Perez E. Bilayers of neutral lipids bear a small but significant charge. European Physical Journal B. 1999; 11(1):127–130.
61. Giasson S, KTL, Israelachvili JN. Adsorption and Interaction Forces of Micellar and Microemulsion Solutions in Ultrathin Films. Langmuir. 1998; 14:891–898.
62. Nagle JF, WMC. Structure of fully hydrated bilayer dispersions. Biochim Biophys Acta. 1988; 942:1–10. [PubMed: 3382651]
63. Watkins EB, Miller CE, Mulder DJ, Kuhl TL, Majewski J. Structure and orientational texture of self-organizing lipid bilayers. Phys Rev Lett. 2009; 102(23)
64. Bassereau P, Pincet F. Quantitative Analysis of Holes in Supported Bilayers Providing the Adsorption Energy of Surfactants on Solid Substrate. Langmuir. 1997; 13:7003–7007.
65. Duncan SL, Larson RG. Comparing Experimental and Simulated Pressure-Area Isotherms for DPPC. Biophysics. 2008; 94(8):2965–2986.
66. Ma G, Allen HC. DPPC Langmuir Monolayer at the Air-Water Interface: Probing the Tail and Head Groups by Vibrational Sum Frequency Generation Spectroscopy. Langmuir. 2006; 22:5341–5349. [PubMed: 16732662]
67. Vanoss, CJ. Interfacial forces in Aqueous Media. Marcel Dekker; New York: 1994.
68. Dufrene Y, LGU. Advances in the characterization of supported lipid films with the atomic force microscope. Biochim Biophys Acta - Biomembranes. 2000; 1509(1–2):14–41.
69. Hui SW, VR, Zasadzinski JA, et al. The structure and stability of phospholipid-bilayers by atomic-force microscopy. Biophys J. 1995; 68(1):171–178. [PubMed: 7711239]

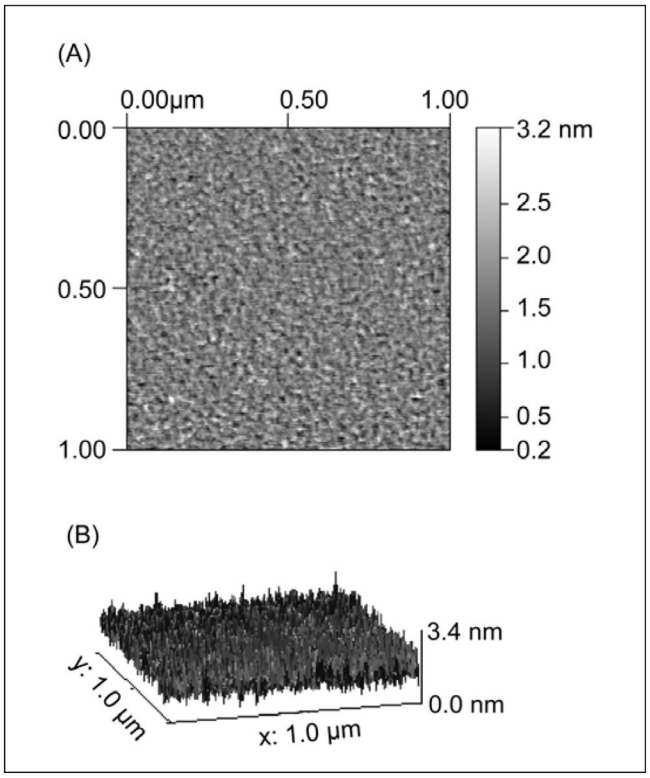

Figure 1.

(A) Representative 1µm × 1µm AFM scans of a SiO_2 e-beam evaporated film on mica in MilliQ water. **(B)** 3D profile of (A). The peak to valley roughness of the film is 31±2Å.

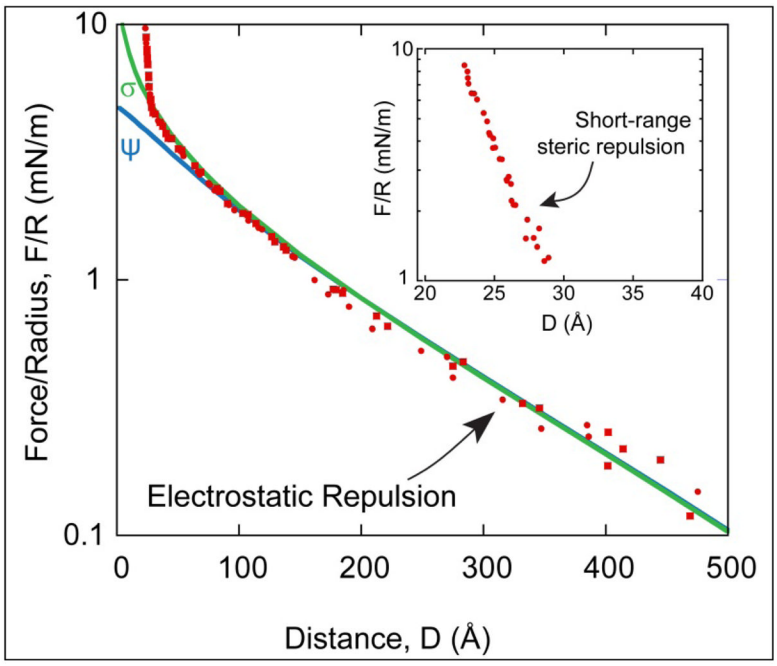

Figure 2.

Force-distance profile between two e-beam evaporated silica films on mica substrates in ~0.5mM KNO_3. Solid lines are electrostatic fits to the data using the Poisson-Boltzman (P-B) equation with constant surface potential $\psi = -107$mV and constant surface charge $\sigma = -9.2$mC/m^2. D = 0 is defined as hard, flattened contact between the silica films (F/R>70mN/m) submerged in water. (Inset) Remaining steric force after subtracting the electrostatic contribution.

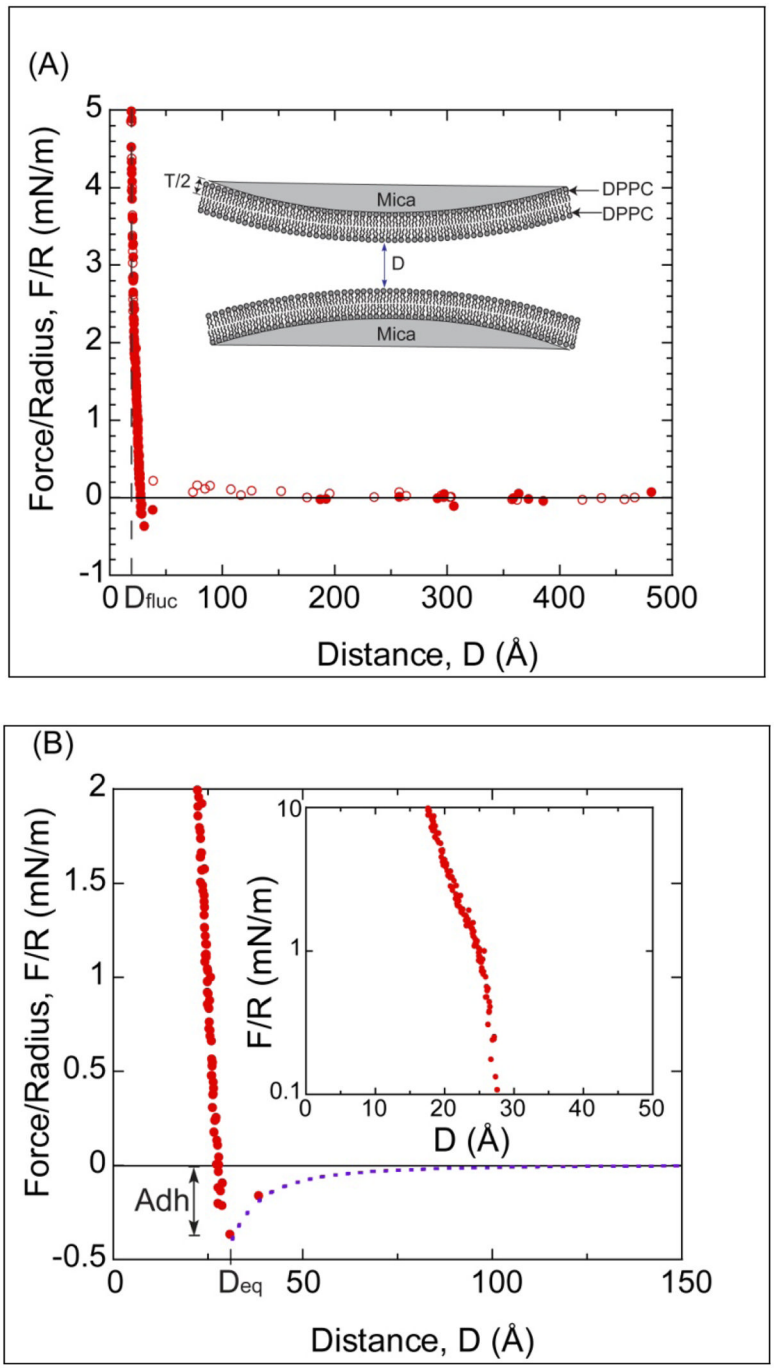

Figure 3.

(A) Force-distance profile between two DPPC bilayers supported on mica in a monovalent solution of 0.5mM KNO_3. Open circles indicate approach and closed circles indicate separation. (Inset) Illustration of the two DPPC membranes on mica, where D=0 is defined as the contact between two non-hydrated DPPC bilayers. T is the thickness of a DPPC leaflet. **(B)** Small range plot of the data in (A) showing the van der Waals interaction $F=-AR/6D^2$ (dash line) with $A=(7\pm1)\times10^{-21}$J. A_{dh} is the magnitude of adhesion force. (Inset) Semi-log plot of the repulsive portion of the force profile.

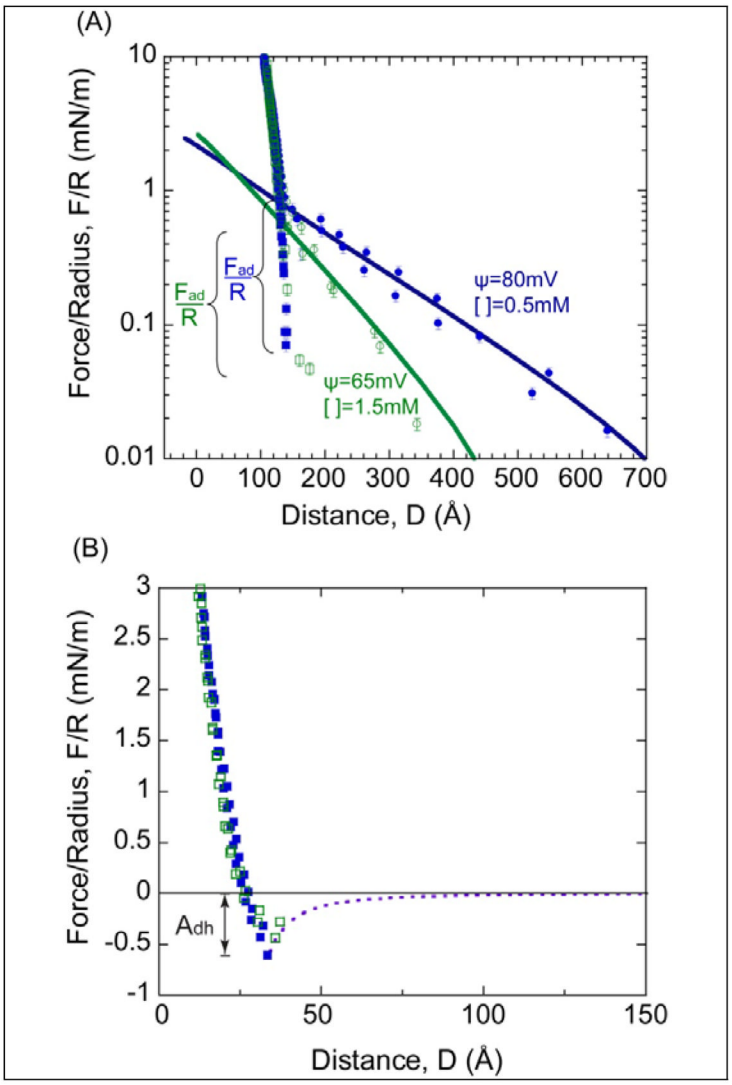

Figure 4.

(A) Measured force profile between DPPC-DPPC membranes supported on SiO_2–covered mica in 0.5mM and 1.5mM KNO_3. D = 0 is defined as contact between bare SiO_2-SiO_2 surfaces in 0.5mM KNO_3. **(B)** Force profile after the electrostatics have been subtracted from the measured force profile in (A). D=0 is based on the contact between two dehydrated DPPC bilayers. Dash line is the theoretical Van der Waals fit ($F=-AR/6D^2$). $A_{dh} = F_{ad}/R$ is the magnitude of the adhesion force.